JOURNAL OF APPLIED ELECTROCHEMISTRY 26 (1996) 1019–1025

Design and performance of a laboratory cell for determination of current efficiency in the electrowinning of aluminium

P. A. SOLLI

Hydro Aluminium, Technology Centre Årdal, P.O. Box 303, N-5870 Øvre Årdal, Norway

T. EGGEN, S. ROLSETH, E. SKYBAKMOEN

SINTEF Materials Technology, Electrolysis Group, N-7034 Trondheim, Norway

Å STERTEN

Department of Electrochemistry, The Norwegian Institute of Technology, N-7034 Trondheim, Norway

Received 20 December 1995; revised 26 July 1996

A new and improved laboratory cell has been specifically designed for determination of current efficiency (CE) as a function of isolated variable parameters in the Hall–Heroult aluminium electrolysis process. The anode is designed to give enhanced and reproducible bubble induced electrolyte convection, while the wettable cathode gives a well defined cathode area, and thus a uniform cathodic current density. Results are given of CE and cathode polarization as functions of cathodic current density, and of CE as a function of interpolar distance. Experiments show reproducible and high values of CE, and low and consistent values of cathode polarization. The CE does not vary for interpolar distances between 10 and 40 mm in the present cell. The cell is well suited for experimental determination of CE as function of electrolyte composition, including impurity concentrations, temperature and current density.

1. Introduction

Industrial production of aluminium is exclusively based on the Hall–Héroult process, involving electrochemical decomposition of alumina (Al_2O_3) dissolved in molten cryolite (Na_3AlF_6) containing additives (usually AlF_3 and CaF_2). The consumable carbon anode liberates CO_2 with a current efficiency close to 100%, while the cathodic current efficiency with respect to aluminium normally ranges from 87 to 96% in commercial cells.

Loss of faradaic efficiency with respect to aluminium in the Hall–Héroult process, and the effect of various parameters on the current efficiency (CE), has been extensively studied for the past few decades. Grjotheim *et al.* [1] have given a review of several of these studies, and it is clear that there are some discrepancies in the available literature as to the quantitative effects of most variables on CE. These discrepancies may be attributed to several factors, including difficulties with the isolation and control of variables both in plant and laboratory studies, differences in cell design, and differences in gas induced or natural convective flow in laboratory cells.

A discussion of rate determining steps and modelling of CE in terms of the cathode processes have been given in previous papers [2, 3]. These papers, based on available literature in the field, conclude that cathodic current is normally consumed by (i) the aluminium deposition reaction, and (ii) reduction reactions with formation of so-called dissolved metal species or reduced entities (RE). The rate determining steps for the aluminium deposition process,

$$AlF_3 + 3Na^+ + 3e^- = Al + 3NaF \qquad (1)$$

are mass transport of aluminium fluoride to the metal surface, and mass transport of sodium fluoride away from the metal surface. In commercial cells there is continuous feed of impurity species to the electrolyte, depressing the concentration of RE to very low equilibrium values in the bulk phase of the electrolyte. Polyvalent impurity species are involved in cyclic redox reactions in the cathode electrode and anode/gas boundary layers.

Modelling of the cathode process and loss of faradaic efficiency [3] predicts that CE is a function of cathodic current density, temperature, electrolyte composition, cathode overvoltage and mass transfer coefficients. In order to determine model parameters, it is necessary to employ a laboratory cell in which it is possible to attain a close to uniform current density, since CE varies with cathodic current density, and thus the geometry of the metal pad. Figure 1 shows examples of two cells with different cathode substrate

0021-891X

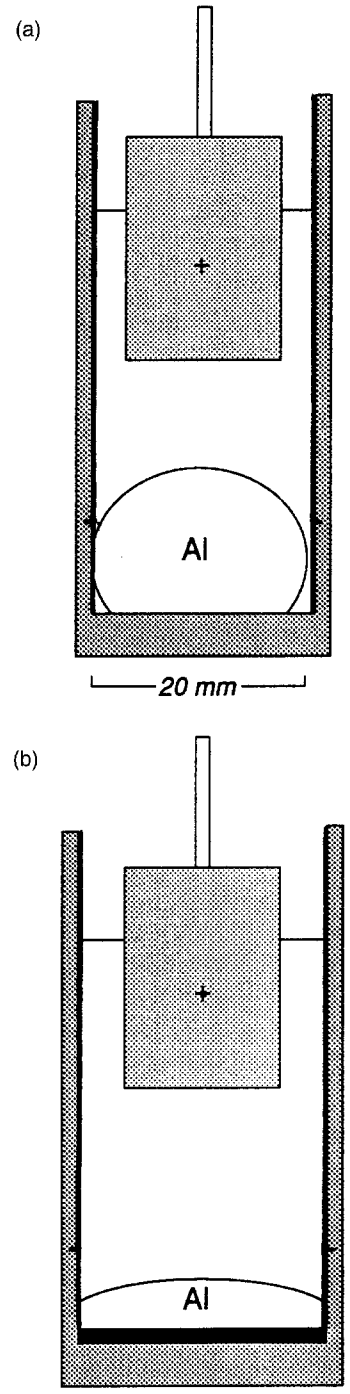

Fig. 1. Metal pad geometries in small scale cells: (a) traditional graphite bottom lining, (b) bottom lining wetted by aluminium.

materials, one with a graphite lining, and one with a wettable cathode. Both cells have electrically shielded side walls (e.g., sintercorundum), so that current is drawn through the bottom of the crucibles. The graphite lining gives an almost spherical metal pad geometry (dependent on cell size), with nonuniform current densities approaching zero on a substantial part of the surface area of the metal pad exposed to electrolyte. The wettable cathode gives a much flatter metal pad surface and, hence, a more well defined and uniform cathodic current density. Determination of CE for the two cells may give quite different results, both with respect to CE levels and parameter dependencies. The convective flow adjacent to the metal pad surface may differ substantially between the two cell configurations, due to the differences in electrode geometry. Also, the interpolar distance is ill-defined for the spherical metal pad geometry in Fig. 1.

For mass transport controlled processes such as the cathode process in aluminium electrolysis cells, the bulk convection will inevitably be of great importance, since it influences the thickness of the diffusion layer and, thus, the rate of mass transport at the electrode. In studies of CE in laboratory cells it is important to attain, not only reproducible convective conditions, but also to have reasonably high rates of electrolyte motion throughout the bulk of the electrolyte. Poor convection may lead to thick diffusion layers and concentration gradients in the bulk electrolyte phase. Conditions in such cells may deviate considerably from commercial cells and erroneous experimentally determined dependencies of CE on variables may result.

2. Experimental details

2.1. *Cell design*

The laboratory cell shown in Fig. 2 was designed specifically with the aim of obtaining good and reproducible convective conditions, and to give an almost flat metal surface (cathode) during electrolysis. Anode, cathode and electrolyte were contained in a graphite crucible with a cylindrical sintercorundum side lining. The anode material was graphite, cylindrically shaped with a vertical hole through the centre. Two horizontal holes were machined normal to each other, and normal to the vertical hole, while the bottom of the anode was shaped with a slight inward slope (11 °) towards the central vertical hole. The idea behind this design was to lead most of the anode gas bubbles up through the central vertical hole, and to set up electrolyte flow out through the horizontal holes, as indicated by the dotted arrows in Fig. 2. The anode

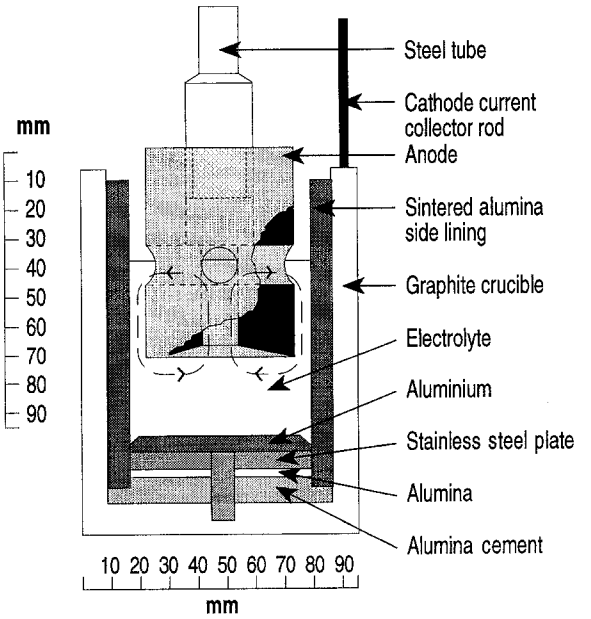

Fig. 2. The laboratory cell with bath circulation pattern indicated by dotted lines and arrows.

was immersed to a level where the electrolyte reached half way up the horizontal holes of the anode.

The cathode was aluminium wetted on a stainless steel plate. This ensured a close to flat aluminium surface, and consequently an even current distribution on the cathode surface. The steel plate rested on a layer of alumina on top of a lining made of high purity cast alumina cement. This arrangement ensured negligible transport of aluminium and electrolyte down to the graphite crucible, and a minimum of metal loss due to formation of aluminium carbide.

2.2. *Determination of current efficiency*

The cell was placed in a vertical tube furnace and positioned to avoid temperature gradients in the electrolyte. The furnace was flushed with argon and a small inert gas flow was maintained through the furnace during the experiments. When the desired temperature was reached, the anode was lowered until electrical contact with the electrolyte was achieved. The anode was then lowered 20 mm further to obtain wanted immersion depth. The temperature of the electrolyte was measured at half-hour intervals during electrolysis, using a Pt–Pt10Rh thermocouple protected by a sintercorundum tube.

The electrolysis current was supplied by a d.c. power supply (Hewlett-Packard, 0–50 A), and monitored as the voltage drop over a standardized resistance (Croydon Precision Instruments, 0.05 Ω, max 50 A) in series with the cell circuit. The cathodic current density was referred to the inner cross-sectional area of the sintercorundum lining. Alumina was supplied to the electrolyte through the central vertical hole of the anode. The duration of each electrolysis experiment was 4 h. Chemicals used were cryolite (Na_3AlF_6, natural handpicked), AlF_3 (Technical grade, sublimated), Al_2O_3, (calcined at 1200 °C) and CaF_2 of high purity.

After electrolysis the furnace, with its contents, were left to cool, after which the crucible was cut open and the solidified metal (Al and Fe) removed and cleaned. The cleaned and dried metal was weighed, and CE calculated from the relation

$$\mathrm{CE}/\% = 100\, m_{\mathrm{Al}}/m_{\mathrm{t}} \qquad (2)$$

where m_{Al} is the mass of metal produced plus 0.33 g (0.9% of theoretical production at 0.85 A cm^{-2}), an assumed loss of metal due to aluminium dissolution after termination of the experiment (20 min until solidification, metal loss estimated to 0.2 g), and due to penetration of sodium into the linings (assumed value 0.13 g of metal). The theoretical amount (weight) of aluminium produced, m_{t}, is given by Faraday's law

$$m_{\mathrm{t}} = ItM_{\mathrm{Al}}/3F \qquad (3)$$

where I is the cell current, t is the electrolysis time, M_{Al} is the molar mass of aluminium, and F is the Faraday constant.

2.3. *Determination of cathode polarization*

An attempt was made to develop a method for determination of cathode polarization in the present laboratory cell. Techniques involving stationary

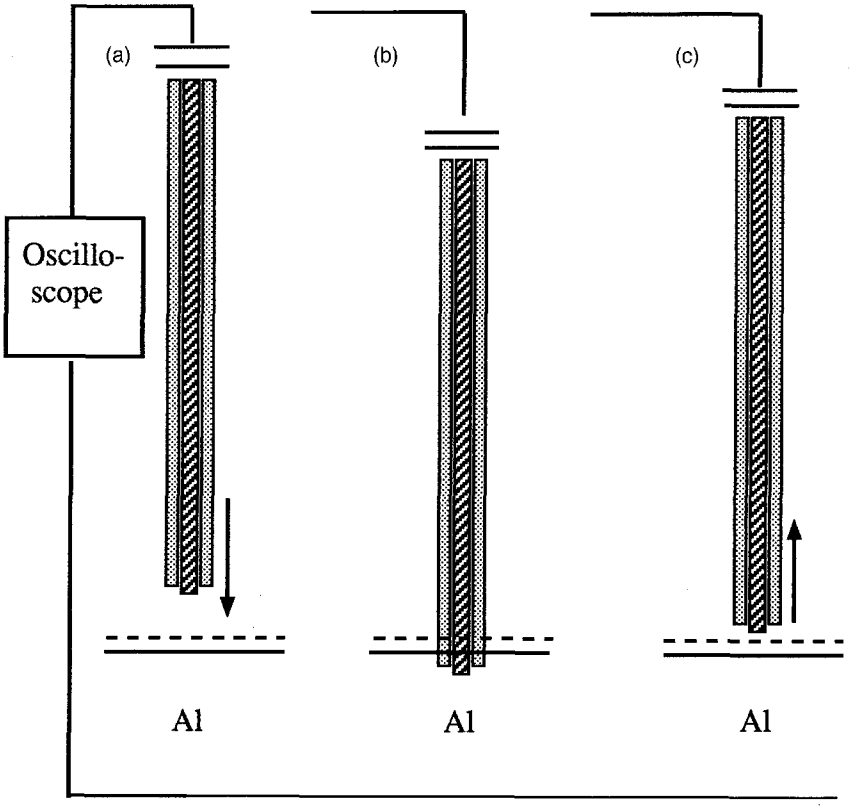

Fig. 3. The principle of cathode polarization measurements. A shielded tungsten probe (a) moved from the electrolyte bulk towards the aluminium cathode (b) immersed into the aluminium pool, and (c) moved out into the bulk electrolyte phase. The potential between probe and aluminium pool is monitored on an oscilloscope.

Al-reference electrodes with isolation of *IR*-drop terms proved difficult to establish with the present cell configuration. A technique described by Rolseth *et al.* [4], based on determination of the sudden transient voltage change when moving a shielded tungsten rod probe in and out of the metal pad, proved successful. The voltage between the Al/W reference electrode (probe) and the cathode current collector rod was monitored on an oscilloscope (Nicolet 3091). The principle of the method is shown in Fig. 3. A motor ensured that the electrode could be moved in and out of the metal pool at variable but constant rate.

Sudden changes of voltage, indicative of the voltage drop over the cathode boundary layer, were attained both when the tungsten electrode achieved electrical contact with the metal phase ('make' sequence) and when the electrode lost contact with the metal pool ('break' sequence). The oscilloscope measurement or sample speed was adjustable.

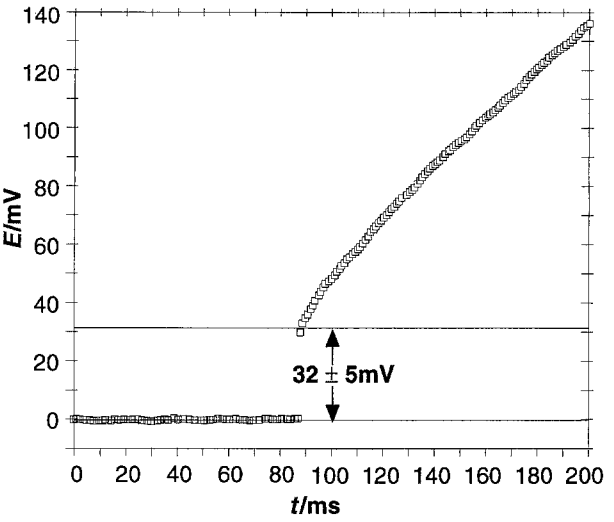

Fig. 4. Transient voltage change during 'break' sequence. Cathodic current density 0.4 A cm^{-2}, temperature 980 °C and voltage jump 32 mV.

3. Results and discussion

3.1. *Cathode polarization*

Usually, the 'make' sequence gave a potential change slightly higher than the 'break' sequence, indicating a drift or error of the Al/W electrode potential. This apparent error seemed to increase with the physical length of the tungsten tip exposed to electrolyte (length of non-shielded tungsten electrode). For unshielded tip lengths less than 2 mm the apparent error seemed to disappear.

A possible theoretical weakness of using the 'break' sequence for determination of the cathode polarization is that aluminium may wet the tungsten and form a meniscus upon leaving the metal phase. When contact between the electrode and metal is lost the potential change may include not only the overvoltage but also an additional *IR* drop. This may lead to an experimentally determined value of polarization more negative than the actual overvoltage during the 'break' sequence, that is, the opposite of what was actually observed. The 'break' sequence gave the lowest and most consistent value of potential change, indicating that the 'break' sequence gives the most representative value of the cathode voltage.

On occasions, problems were encountered with ill-defined voltage changes. In most cases this problem was overcome by adjusting the oscilloscope measurement speed, but the observations confirmed the uncertain nature of such measurements. Oscilloscope measurement/sample speeds in the range 10^{-4} to 10^{-5} s proved to give the most easily interpretable results.

Figure 4 shows an example of voltage change during a 'break' sequence at cathodic current density 0.4 A cm^{-2} with a voltage jump (polarization) reading of 32 mV. In most cases several consecutive measurements of voltage jumps showed standard deviations from the average of roughly 10–20%. Excessively high or irregular transient potential jumps were occasionally observed for excessively worn sinter-corundum shieldings or for inadequately shielded, or poorly prepared, probes. In the following the cathode polarization is assumed to be adequately described as the average of more than 10 consecutive voltage jump measurements during the 'break' sequence.

Cathode polarization was determined as a function of current density for an electrolyte with NaF/AlF_3 molar ratio 2.5, 5 wt % CaF_2, 4 wt % alumina and temperature 980 °C. The results are given in Fig. 5, together with some values at NaF/AlF_3 molar ratio 1.0 (40 wt % AlF_3 in excess of the cryolite composition). Each experimental value in the Figure represents the average of 10–20 consecutive measurements.

For NaF/AlF_3 molar ratio 2.5 the cathodic polarization roughly follows a linear relationship in the current density range of industrial interest, with a regression line of

$$\eta/\mathrm{V} = -0.086\, i_c \qquad (4)$$

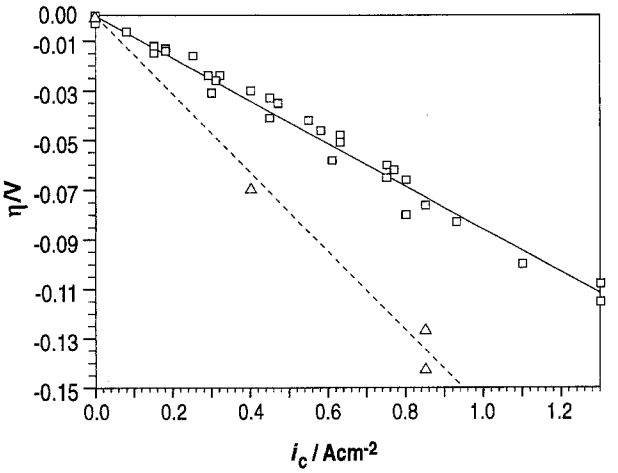

Fig. 5. Cathode polarization as a function of cathodic current density at NaF/AlF_3 molar ratio (□) $r = 2.5$ and (△) $r = 1.0$. Points: Experimental values, lines: regression.

where i_c is the cathodic current density (A cm^{-2}). The standard error in the regression slope is 3%. The regression line for NaF/AlF_3 molar ratio 1.0 is,

$$\eta/V = -0.158\, i_c \quad (5)$$

but is based on only four average values, see Fig. 5. The results show that the polarization becomes more negative with decreasing NaF/AlF_3 ratio, in general agreement with literature data [1, 5].

The polarization values determined in the present laboratory cell are low, indicating that the laboratory cell functions well with respect to convective flow close to the cathode. However, the present method is, as previously mentioned, not ideal, in that it may give somewhat variable results dependent of interpretation, and that the probe disrupts and interferes with the boundary layer. Great care was needed when preparing the tungsten probes.

Despite the somewhat high standard deviation of 10–20 consecutive runs (10–20%), the mean values were quite reproducible, as indicated by the low scatter of points in Fig. 5. The standard deviation from the regression line is less than 5 mV for NaF/AlF_3 molar ratio 2.5.

The polarization values found in the present laboratory cell are roughly the same as those found in commercial cells [4] for comparable current densities, which indicates that the concentration gradients and diffusion layer thicknesses are of comparable magnitudes.

3.2. *Current efficiency*

3.2.1. CE and reproducibility. Initial experiments were carried out with NaF/AlF_3 molar ratio 2.5, 5 wt % CaF_2, 4 wt % alumina, temperature 980 °C, and cathodic current density 0.85 A cm^{-2}. The results from four experiments showed good reproducibility, with mean CE 93.0% and absolute standard deviation 0.2%. The above alumina content was based on the initial weighed in amount. This may deviate somewhat from the real concentration due to gradual dissolution of the sintercorundum side lining. Analysis of samples taken during experiments gave alumina concentrations in the range 4 to 6 wt %.

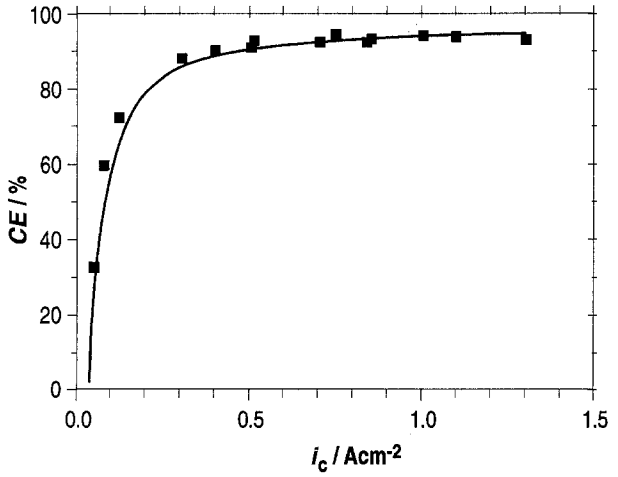

Fig. 6. Current efficiency, CE, as a function of cathodic current density, i_c. Temperature 980 °C, NaF/AlF_3 molar ratio 2.5, 5 wt % CaF_2 and 4 wt % Al_2O_3. Experimental values (points) and fitted curve.

3.2.2. CE and cathodic current density. Current efficiency was determined as a function of cathodic current density for an electrolyte with NaF/AlF_3 molar ratio 2.5, 5 wt % CaF_2, 4 wt % alumina and temperature 980 °C. The results are given in Fig. 6. The mass transfer conditions at the cathode may have changed slightly with current density due to variations in the anode gas induced convection.

The results show that CE decreases with decreasing cathodic current density, especially towards zero current. The advantage of the present cell configuration is that CE as a function of the *isolated* cathodic current density parameter can be obtained, due to the uniform current distribution on the aluminium pad surface. In industrial cells the current efficiency is a function of location on the metal surface, both due to lower values of cathodic current density in the side channels towards the side ledge and due to enhanced gas induced convection in the channels. The result may be that the local CE on the cathode surface beneath the anodes is considerably higher than for the surface area in the side channels. For estimation of the loss in the side channels of industrial cells it is necessary to obtain values of the *local* CE as a function of *local* current density. The results from the present laboratory cell may be particularly useful in order to evaluate the average CE in commercial cells, and to evaluate the CE losses due to variable side channel widths.

An earlier version of the present cell configuration [7, 8], but without the wettable cathode, gave CE values 10–13% lower than in the present study for roughly the same experimental conditions. This was probably due to the non-uniform current distribution and formation of aluminium carbide, as the aluminium rested directly on the bottom of the graphite crucible.

The use of a stainless steel plate as cathode substrate inevitably leads to iron dissolution into the molten aluminium phase. Analysis of the metal pool after electrolysis revealed an iron concentration of 6–8 wt % Fe, roughly in agreement with equilibrium values [9]. The alloy composition corresponds to an activity of aluminium of roughly 0.93, a deviation from unit activity which is expected not to influence the CE to any appreciable extent.

3.2.3. CE and interpolar distance. Results from an investigation of current efficiency as a function of interpolar distance in the present laboratory cell is obviously not quantitatively representative of industrial cells, due to the differences in scale, anode gas bubble size, and metal pad instability or wave motion. Nonetheless, the results may give an indication of laboratory cell performance and give information concerning rate determining factors for the loss process.

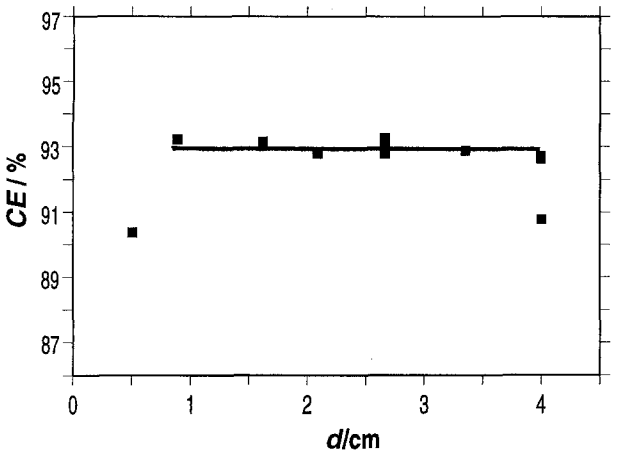

Fig. 7. Current efficiency, CE, as a function of interpolar distance, d. Temperature 980 °C, NaF/AlF_3 ratio 2.5, 5 wt % CaF_2, 4 wt % Al_2O_3 and cathodic current density 0.85 A cm^{-2}. Points: experimental values, solid horizontal line: constant 93.0% CE.

The anode to cathode distance was varied between 0.6 and 4.0 cm, with the same bath composition and temperature as in the investigation of CE as a function of current density, and constant anode immersion depth for all interpolar distances. The results given in Fig. 7 show that CE is roughly constant for distances greater than, or equal to, 1.0 cm. The one low CE value obtained, at $d = 4.0$ cm, is hard to explain, and two other runs at the same distance gave CE values roughly the same as for lower interpolar distances. The low value at $d = 0.6$ cm is probably due to direct contact between anode gas bubbles and the electrolyte/metal interface, giving a substantially higher rate of metal loss than for greater interpolar distances. During electrolysis the anode was consumed and worn at a similar rate as the buildup of aluminium, giving close to constant interpolar distance during each experiment.

The results show that for the present cell, any interpolar distance between 10 and 35 mm can be chosen without influencing the current efficiency. The cell seems to give well defined bulk convective flow conditions, so that a change in interpolar distance does not significantly alter the mass transport rates in the cathode boundary layer and the CE.

3.3. *Observations*

Figure 8 shows photographs of two cell halves, cut open after solidification and cooling. The figure shows that the cathode surface has a reasonably low curvature and the cathodic current distribution must have been quite uniform, especially for intermediate and high interpolar distances. The sintercorundum side lining shows considerable wear near the horizontal holes in the anode, indicating enhanced electrolyte flow from inside the anode towards the side lining. Thus the anode gas seems to set up a well defined electrolyte circulation flow.

4. Conclusion

The present laboratory cell design gives reproducible and high values of CE, probably due to the wettable flat cathode with uniform current distribution, and due to reproducible and sufficiently good convective conditions. The cell is more likely to represent industrial conditions than traditional small-scale laboratory cells and seems to be well suited for determination of CE as function of isolated variable parameters such as bath composition, temperature, current density, and electrolyte impurity concentrations.

Acknowledgement

Financial support from The Research Council of Norway and from Norwegian aluminium industry is gratefully acknowledged.

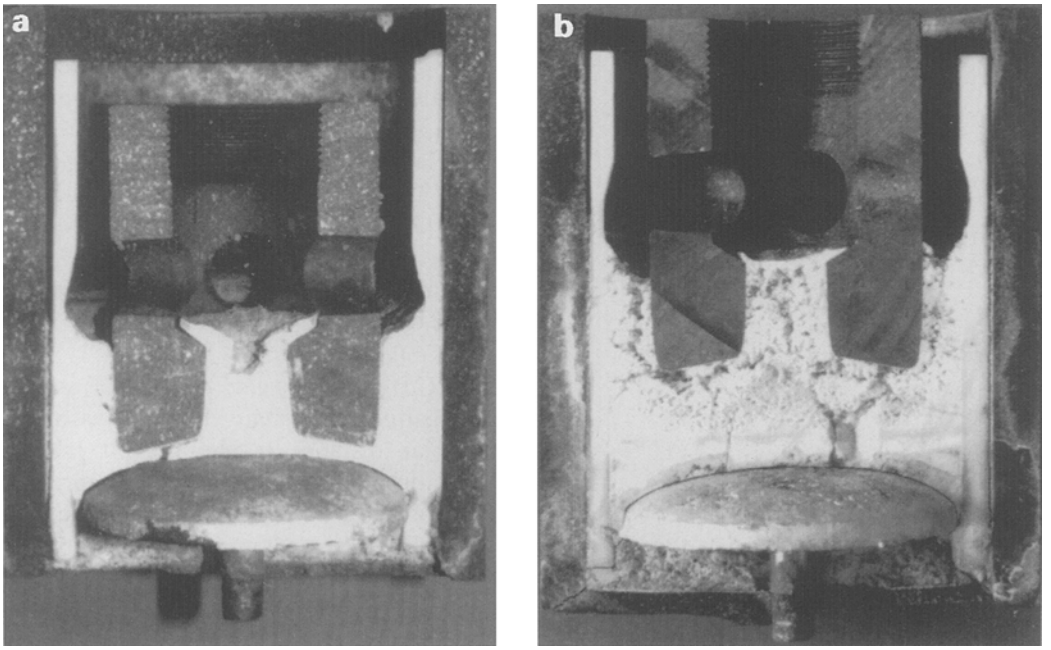

Fig. 8. Photograph of dissected cells with (a) interpolar distance 6 mm, and (b) interpolar distance 27 mm.

References

[1] K. Grjotheim, C. Krohn, M. Malinovsky, K. Matiasovsky and J. Thonstad, 'Aluminium Electrolysis. Fundamentals of the Hall–Héroult Process', 2nd edn, Aluminium-Verlag, Dusseldorf (1982), chapter 9.

[2] Å. Sterten and P. A. Solli, *J. Appl. Electrochem* **25** (1995) 809.

[3] Å. Sterten and P. A. Solli, *ibid* **26** (1996) 187.

[4] S. Rolseth, A. Solheim and J. Thonstad, 'Proceedings of the International Symposium on Reduction and Casting of Aluminium' (edited by C. Bickert), vol. 6, The Metallurgical Society of the Canadian Institute of Mining and Metallurgy, Pergamon Press, Montreal (1988), p. 229.

[5] J. Thonstad and S. Rolseth, *Electrochim. Acta* **23** (1978) 221.

[6] M. W. Chase, C. A. Davies, J. R. Downey, D. J. Frurip, R. A. McDonald and A. N. Syverud, 'JANAF Thermochemical Tables', 3rd. edn, *J. Phys. Chem. Ref. Data*, **14**, Suppl. 1 (1985).

[7] A. Solheim, Å. Sterten, S. Rolseth, E. Skybakmoen, A. Røstum and J. Thonstad, 'Proceedings of the 6th Czechoslovak Aluminium Symposium', Banska Bystrica, Czechoslovakia (1988), p. 184.

[8] Å. Sterten, S. Rolseth, E. Skybakmoen, A. Solheim and J. Thonstad, 'Light Metals' (edited by L. G. Boxall), Proceedings of 117th TMS Annual Meeting (1988) p. 663.

[9] T. B. Massalski, J. L. Murray, L. H. Bennett and H. Baker, 'Binary Alloy Phase Diagrams', vol. 1, Am. Soc. Met., OH (1986), p. 112.